An aerial photograph of a university campus, likely the University of Michigan, with a blue tint. The image shows various buildings, a central tower, and parking lots. The text is overlaid on the top half of the image.

Modeling the Background Environment of CMEs/Flares

Bart van der Holst



ATMOSPHERIC, OCEANIC
AND SPACE SCIENCES

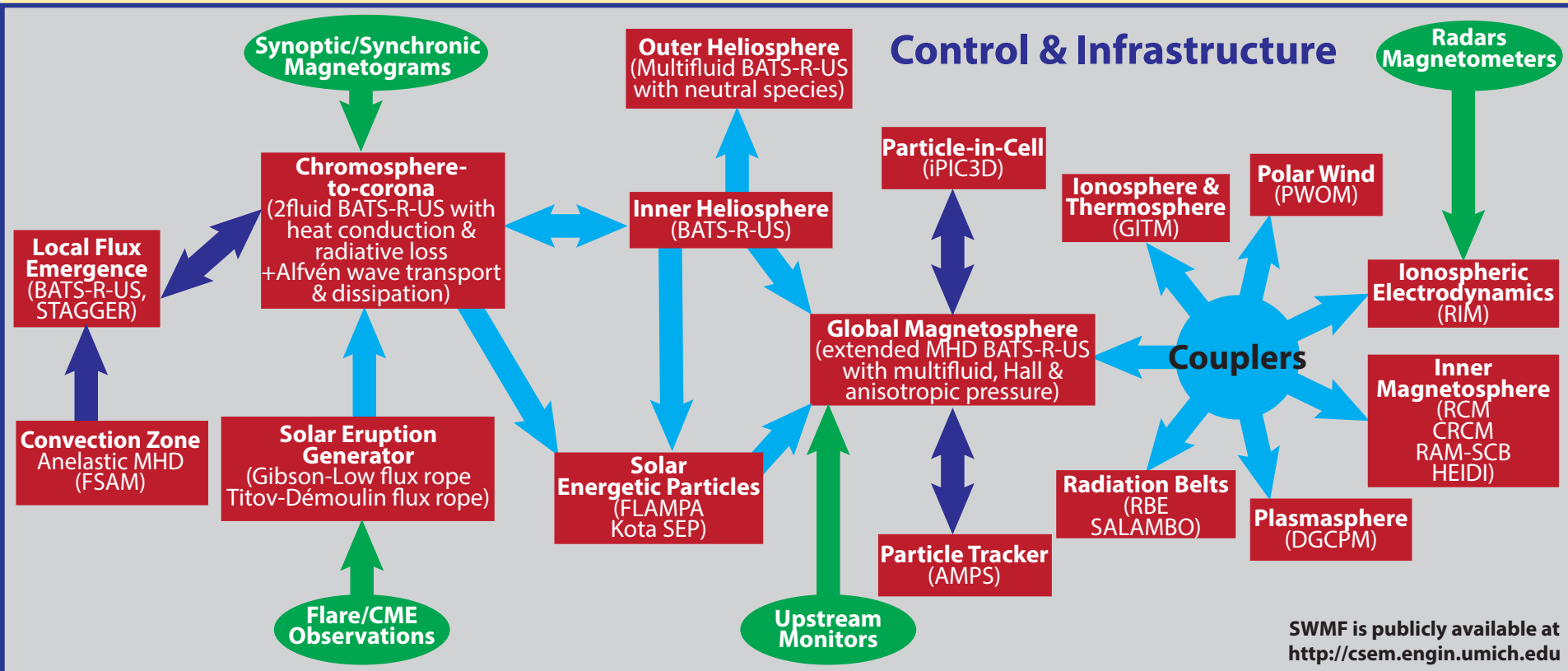
UNIVERSITY of MICHIGAN

- M Space Weather Modeling Framework (SWMF)**
- M New solar corona and inner heliosphere model with low-frequency Alfvén wave turbulence**
- M Validation: EUV images**
- M Temperature anisotropy and plasma instabilities**
- M Validation: 1AU in-situ**
- M Validation: Charge state**

Space Weather Modeling Framework (SWMF)



Block Diagram of the Space Weather Modeling Framework



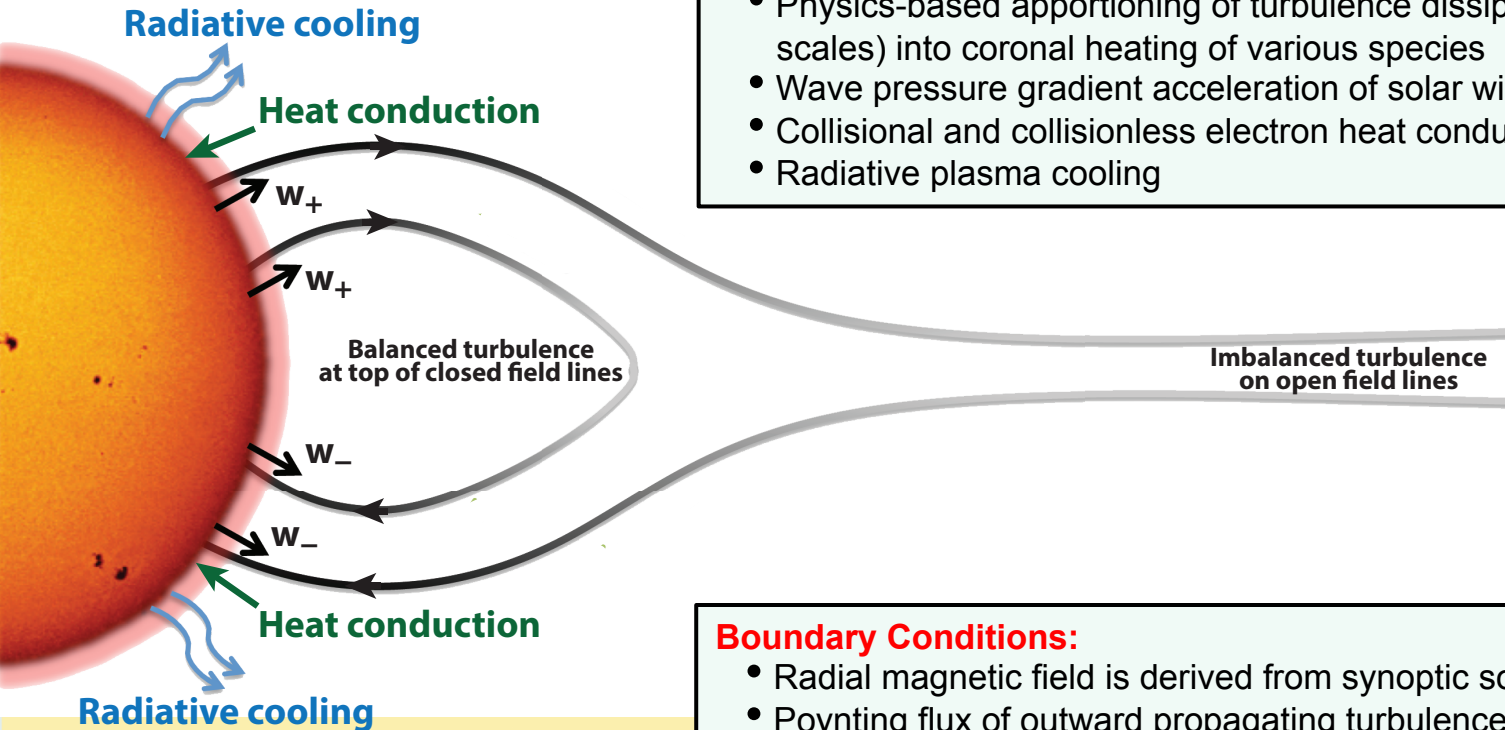
Alfvén Wave Solar Model (AWSoM)



van der Holst et al. ApJ **782**, 81 (2014).

XMHD physics:

- Separate $T_{p\parallel}$, $T_{p\perp}$ and T_e
- WKB equations for parallel and antiparallel propagating turbulence (w_{\pm})
- Non-WKB physics-based reflection of w_{\pm} results in turbulent cascade
- Correction for presumed uncorrelated waves w_{\pm} in the balanced turbulence near apex of closed field lines
- Physics-based apportioning of turbulence dissipation (at the gyro-radius scales) into coronal heating of various species
- Wave pressure gradient acceleration of solar wind plasma
- Collisional and collisionless electron heat conduction
- Radiative plasma cooling



Boundary Conditions:

- Radial magnetic field is derived from synoptic solar magnetograms
- Poynting flux of outward propagating turbulence:

$$(S_A / B) = 1.1 \times 10^6 \text{ Wm}^{-2} \text{ T}^{-1}$$

(This Poynting flux is based on Hinode observations by B. De Pontieu)

Alfvén Wave Turbulence

M Wave energy densities of counter-propagating transverse Alfvén waves parallel (+) and anti-parallel (-) to magnetic field (similar to Matthaeus et al., 1999):

$$\frac{\partial w_{\pm}}{\partial t} + \nabla \cdot [(\mathbf{u} \pm \mathbf{V}_A) w_{\pm}] + \frac{w_{\pm}}{2} (\nabla \cdot \mathbf{u}) = \mp \mathcal{R} \sqrt{w_- w_+} - \Gamma_{\pm} w_{\pm}$$

energy reduction in expanding flow
wave dissipation

Alfvén wave advection
wave reflection

M Phenomenological cascade rate (Dmitruk et al., 2002): $\Gamma_{\pm} = \frac{2}{L_{\perp}} \sqrt{\frac{w_{\mp}}{\rho}}$

M Similar to Hollweg (1986), we use a simple scaling law for the transverse correlation length $L_{\perp} \sqrt{B} = 150 \text{ km T}^{1/2}$

Wave Reflection

M Wave reflection rate:

$$\mathcal{R} = \min \left[\sqrt{[(\mathbf{V}_A \cdot \nabla) \log V_A]^2 + (\mathbf{b} \cdot [\nabla \times \mathbf{u}])^2}, \max(\Gamma_{\pm}) \right] \begin{cases} \left(1 - 2\sqrt{\frac{w_-}{w_+}}\right) & \text{if } 4w_- \leq w_+ \\ 0 & \text{if } \frac{1}{4}w_- \leq w_+ \leq 4w_- \\ \left(2\sqrt{\frac{w_+}{w_-}} - 1\right) & \text{if } 4w_+ \leq w_- \end{cases}$$

Limit rate in transition region

Alfvén speed gradient and field-aligned vorticity

In balanced turbulence, the reflection rate does not affect the cascade rate and may be neglected (derivation assumed that one wave is dominant)

M Key features of reflection term $\mp \mathcal{R} \sqrt{w_- w_+}$

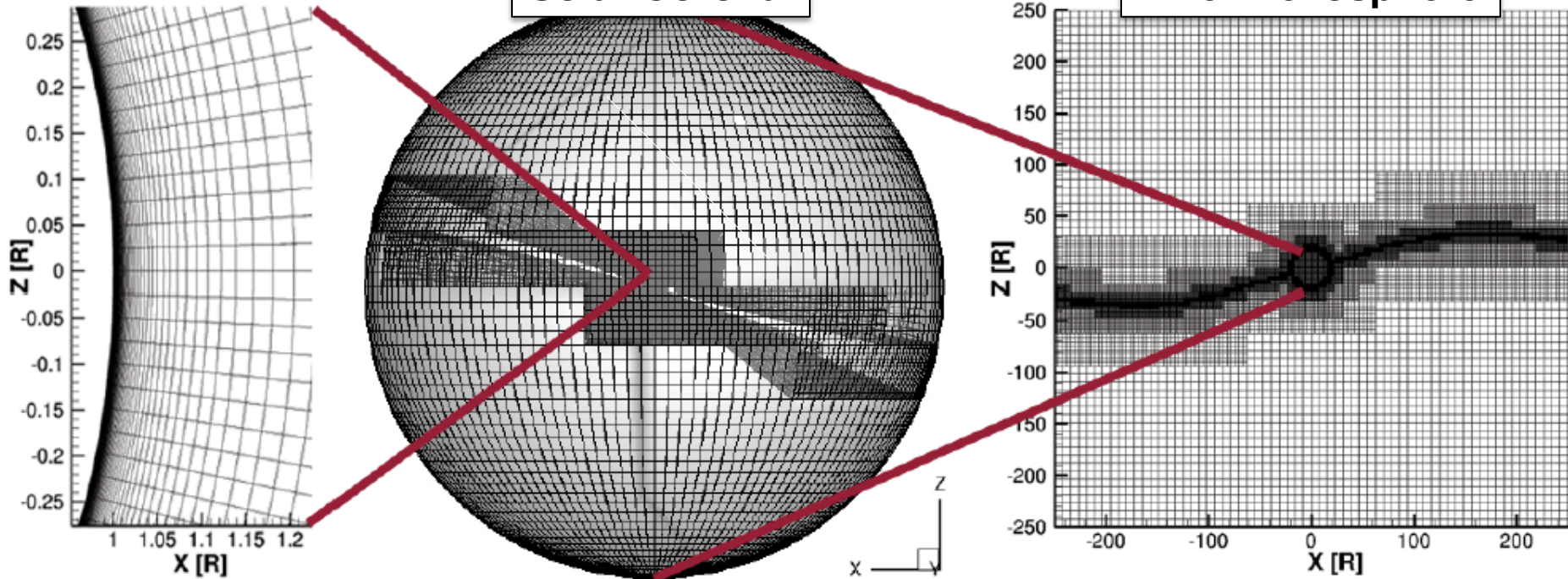
- Wave reflection turns to zero in balanced turbulence
- Sign is such that amplitude of dominant wave reduces, and enhances the counter-propagating minor wave (while conserving energy)
- Magnitude of reflection is mostly controlled by Alfvén speed gradients

- M Counter-propagating Alfvén waves due to partial reflection of waves**
- M Non-linear interaction of counter-propagating waves results in transverse energy cascade**
- M Cascade of Alfvén waves transitions into cascade of kinetic Alfvén waves (KAW)**
- M Dissipation of KAW at gyro-radius scale or smaller**
- M Heat partitioning formulas (Chandran et al., 2011):**
 - 🌐 Linear damping of KAW, resulting in **electron** and **parallel proton** heating
 - 🌐 Nonlinear damping of KAW via stochastic heating of protons, resulting in **perpendicular proton** heating
 - 🌐 **Electron** heating at scales much smaller than proton gyro-radius

Computational Grids

Solar Corona

Inner Heliosphere

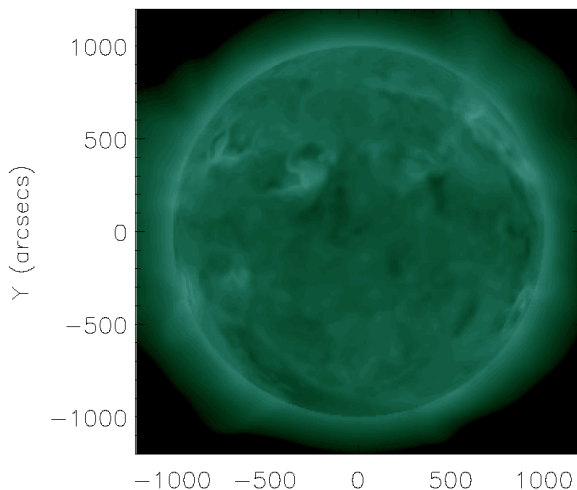


- M** ASoM is split in two coupled framework components: stretched spherical grid for solar corona, Cartesian grid for inner heliosphere
- M** Significant grid stretching to grid resolve the upper chromosphere and transition region in addition to artificial transition region broadening (Lionello et al. 2009, Sokolov et al. 2013)
- M** AMR to resolve the heliospheric currentsheets

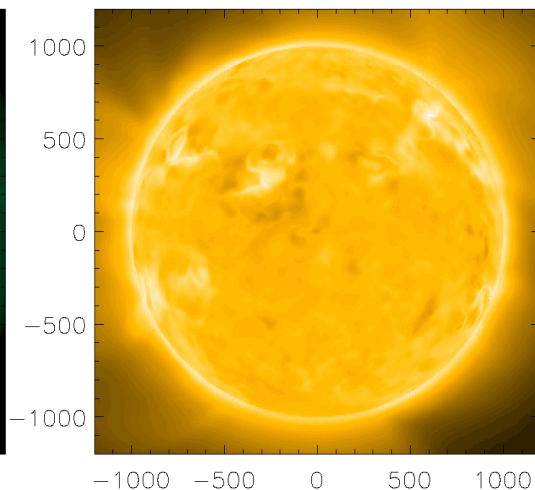
Validation: EUV Images for CR2107



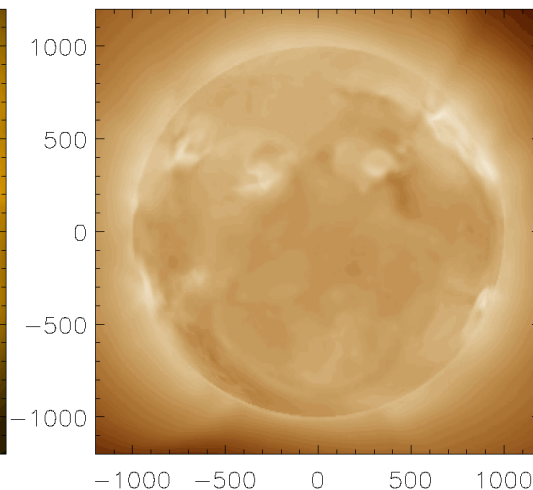
Model AIA 94



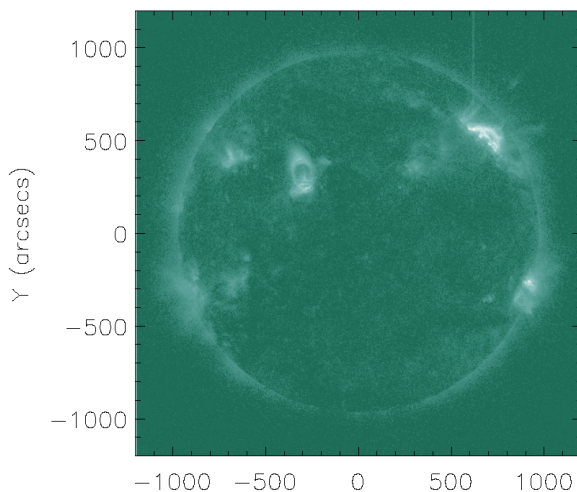
Model AIA 171



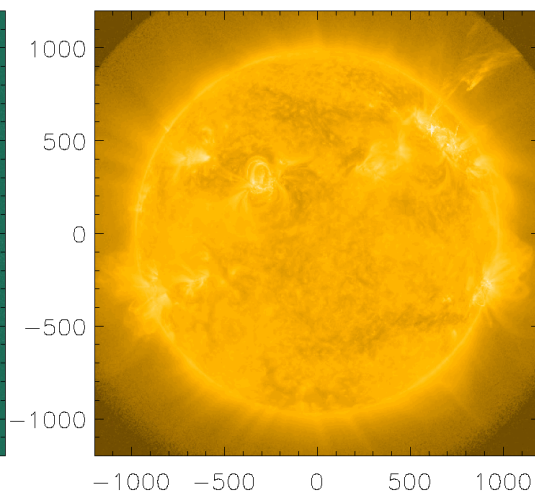
Model AIA 193



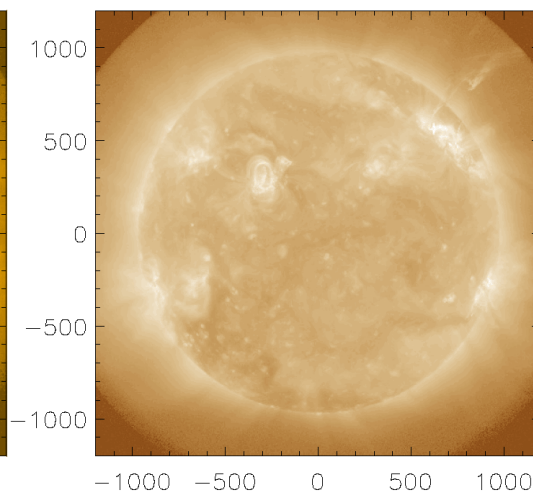
SDO AIA 94



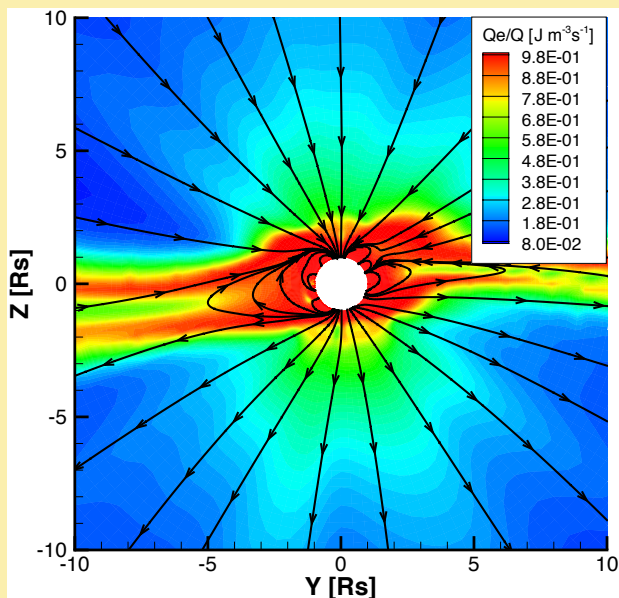
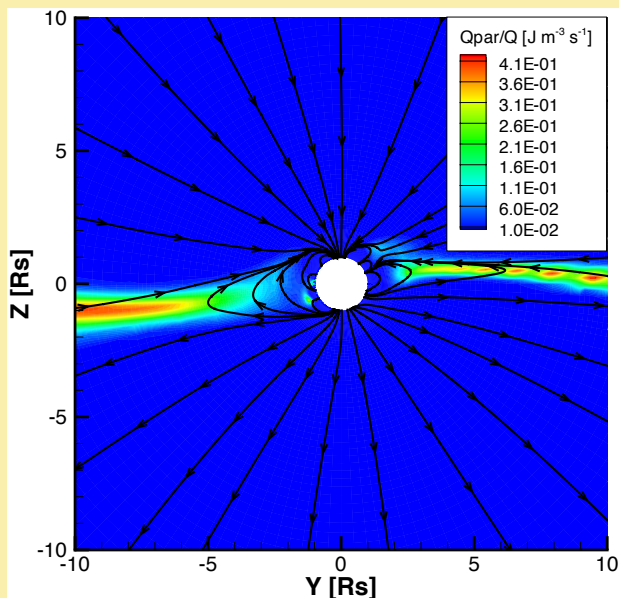
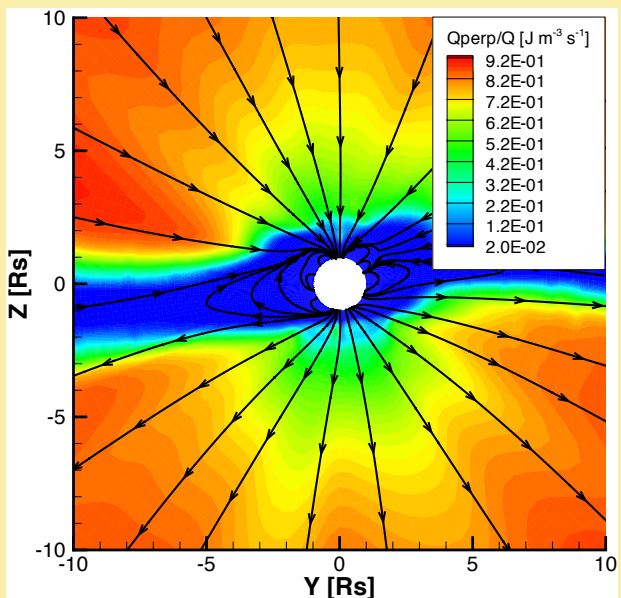
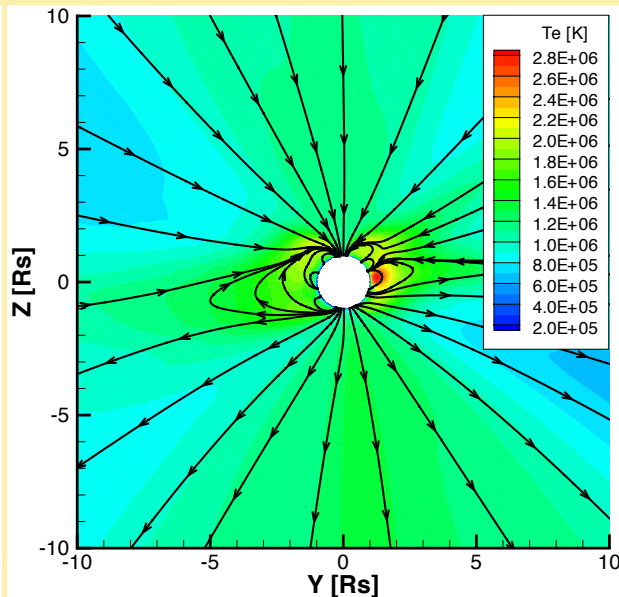
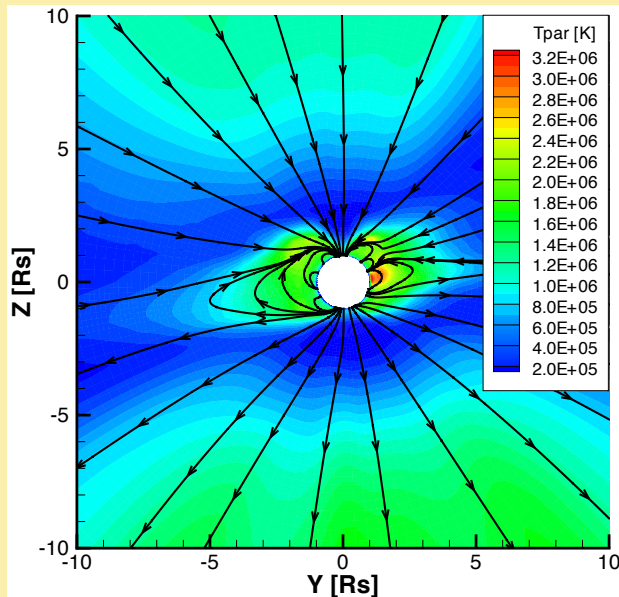
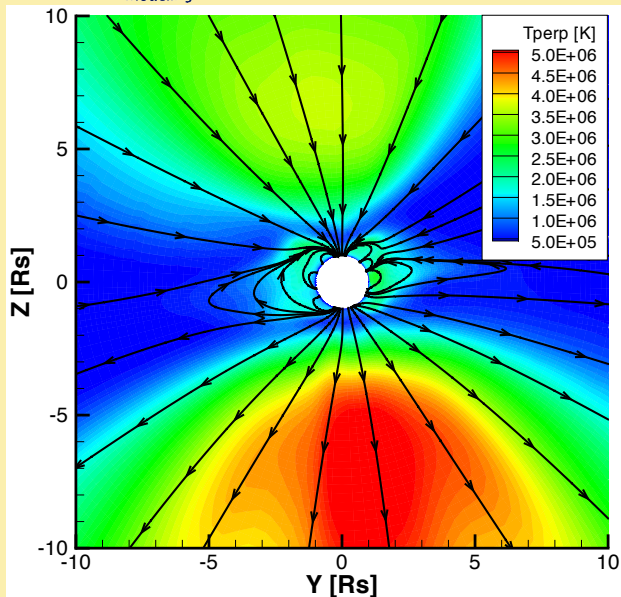
SDO AIA 171



SDO AIA 193



Heat Partitioning for the Electron and Anisotropic Proton Temperatures



Limiting the Anisotropic Pressure

X. Meng et al. 2012 JCP, JGR

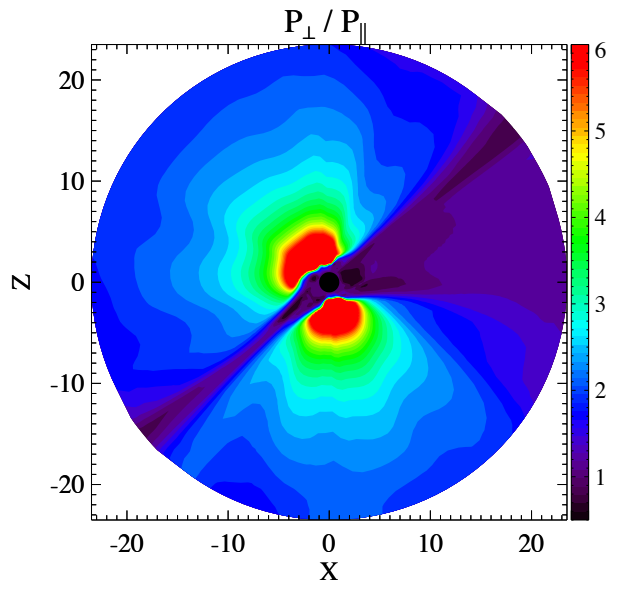
The instability-based anisotropic pressure relaxation towards the marginal stable pressure $\overline{p_{\parallel}}$ while keeping averaged pressure p unmodified:
$$\frac{\delta p_{\parallel}}{\delta t} = \frac{\overline{p_{\parallel}} - p_{\parallel}}{\tau}$$

applied in firehose, mirror and proton cyclotron unstable regions. τ is taken to be the inverse of the growth rates of the instabilities (Hall 1979, 1980, 1981 and Southwood & Kivelson 1993):

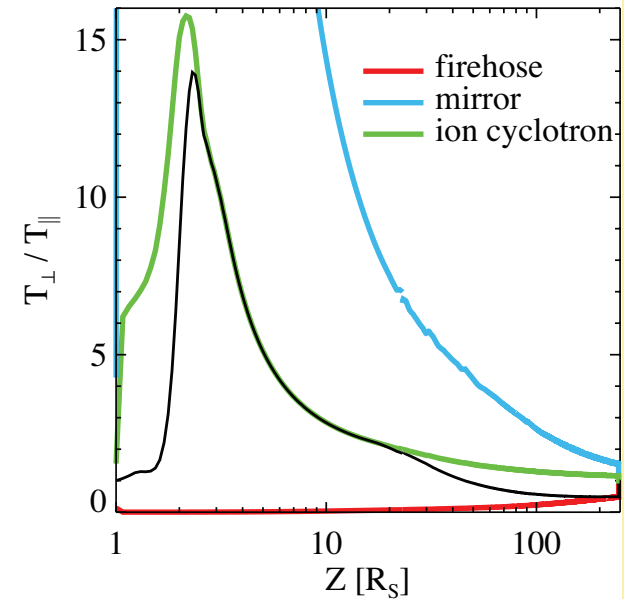
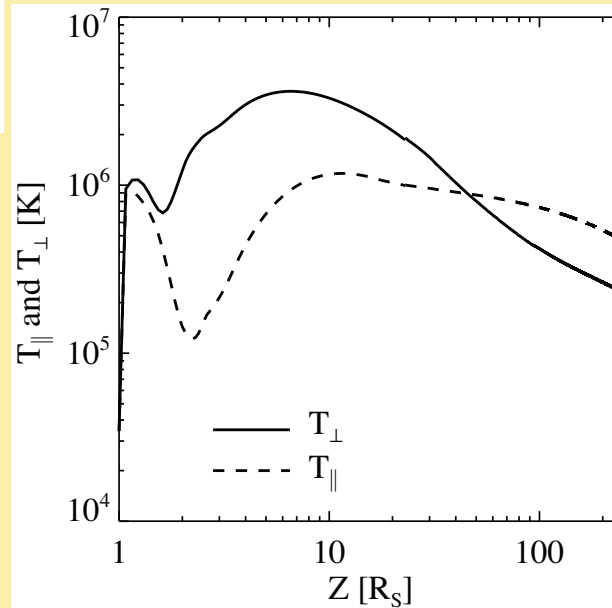
	instability criteria	relaxation time τ
firehose	$\frac{p_{\parallel}}{p_{\perp}} > 1 + \frac{B^2}{\mu_0 p_{\perp}}$	$\tau_f = \frac{1}{\gamma_{fFLR}(\lambda_f)} = \frac{2}{\Omega_i} \frac{\sqrt{p_{\parallel}(p_{\perp} - p_{\parallel}/4)}}{\Delta p_f}$
mirror	$\frac{p_{\perp}}{p_{\parallel}} > 1 + \frac{B^2}{2\mu_0 p_{\perp}}$	$\tau_m = \frac{1}{\gamma_m(\lambda_m)} = \frac{3\sqrt{5}}{4\Omega_i} \sqrt{\frac{p_{\parallel}}{2\Delta p_m}}$
proton cyclotron	$\frac{p_{\perp}}{p_{\parallel}} > 1 + 0.3 \sqrt{\frac{B^2}{2p_{\parallel}}}$	$\tau_{ic} = \frac{10^2}{\Omega_i}$

X. Meng et al., submitted to ApJ

Temperature anisotropy in the simulated Y=0 meridional slice



Temperature anisotropy along the north axis

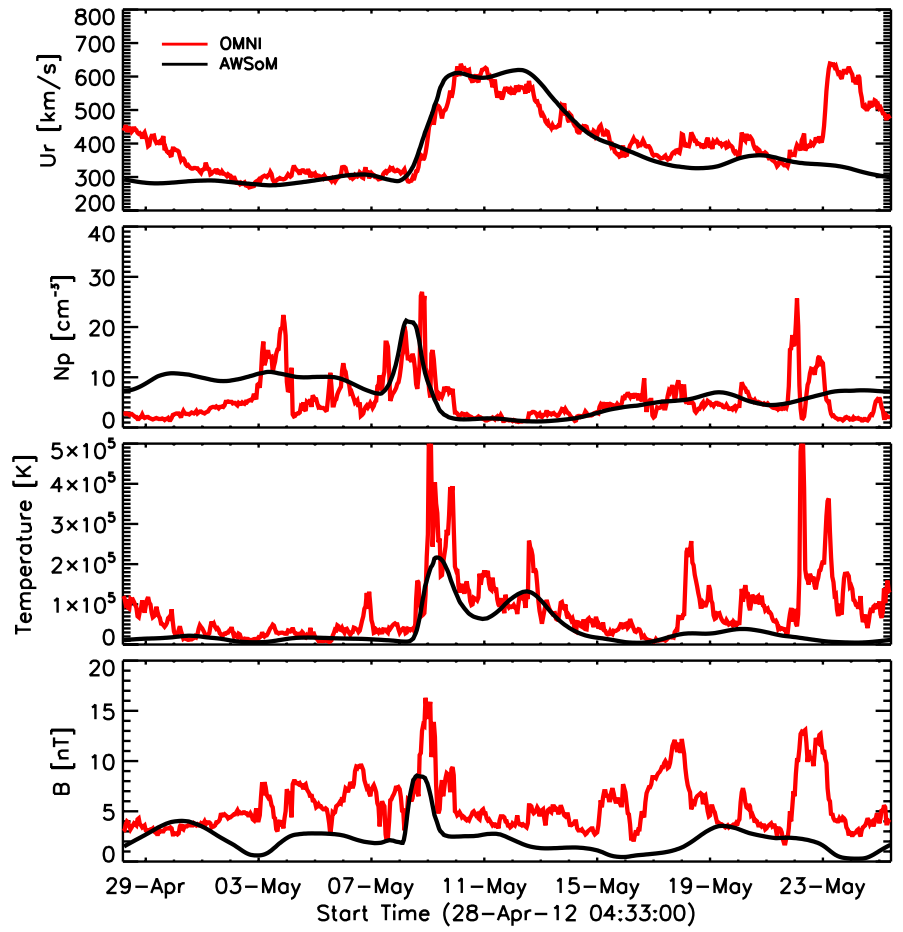
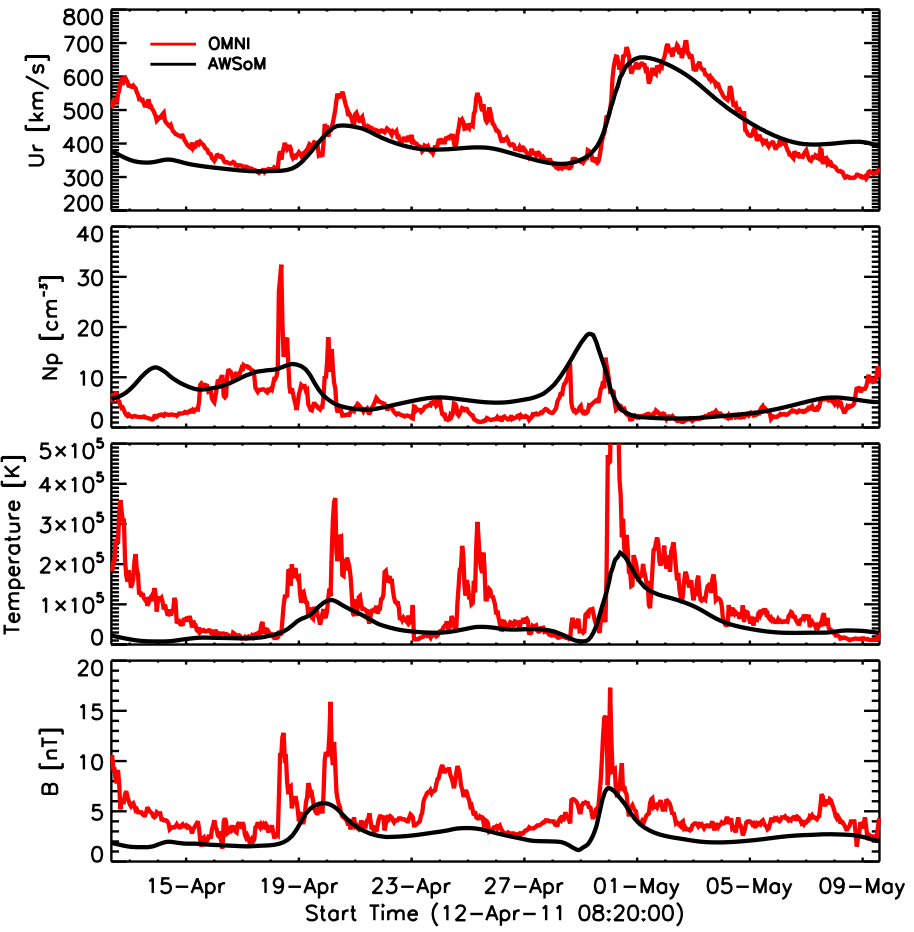


Validation at 1AU

ACE versus AWSoM

CR2109

CR2123

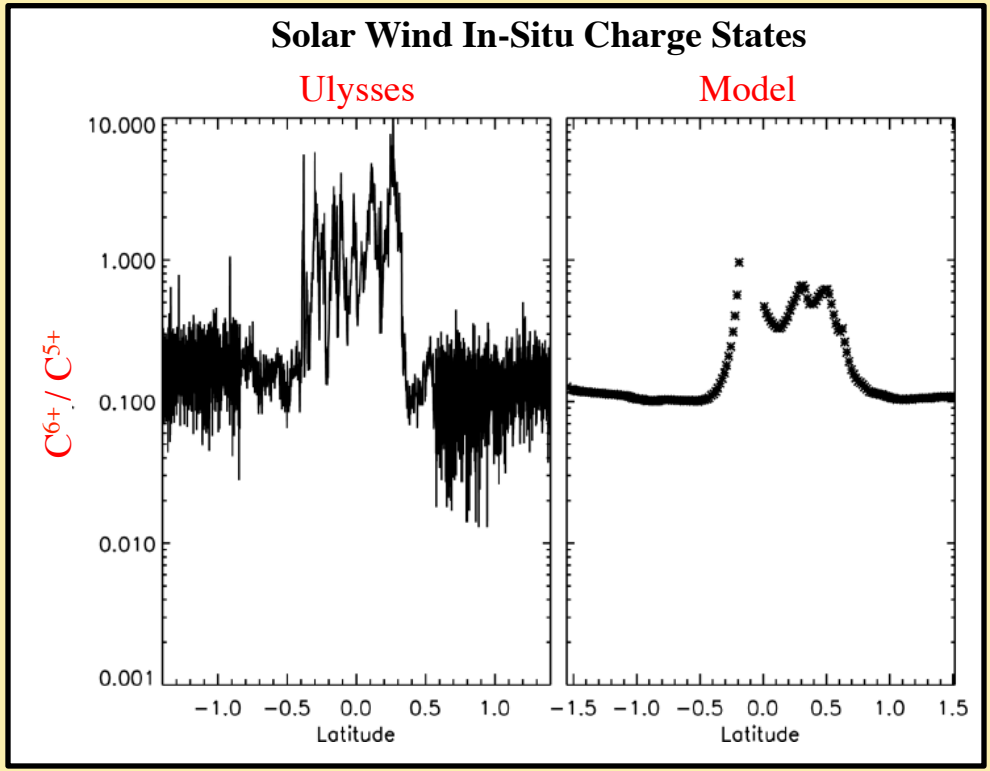
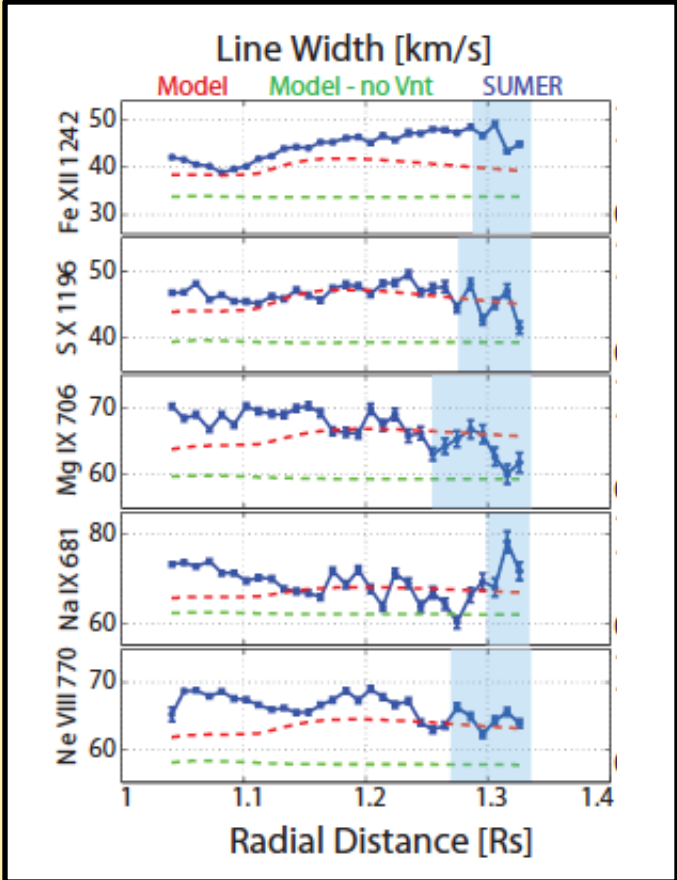


Validation: Charge State



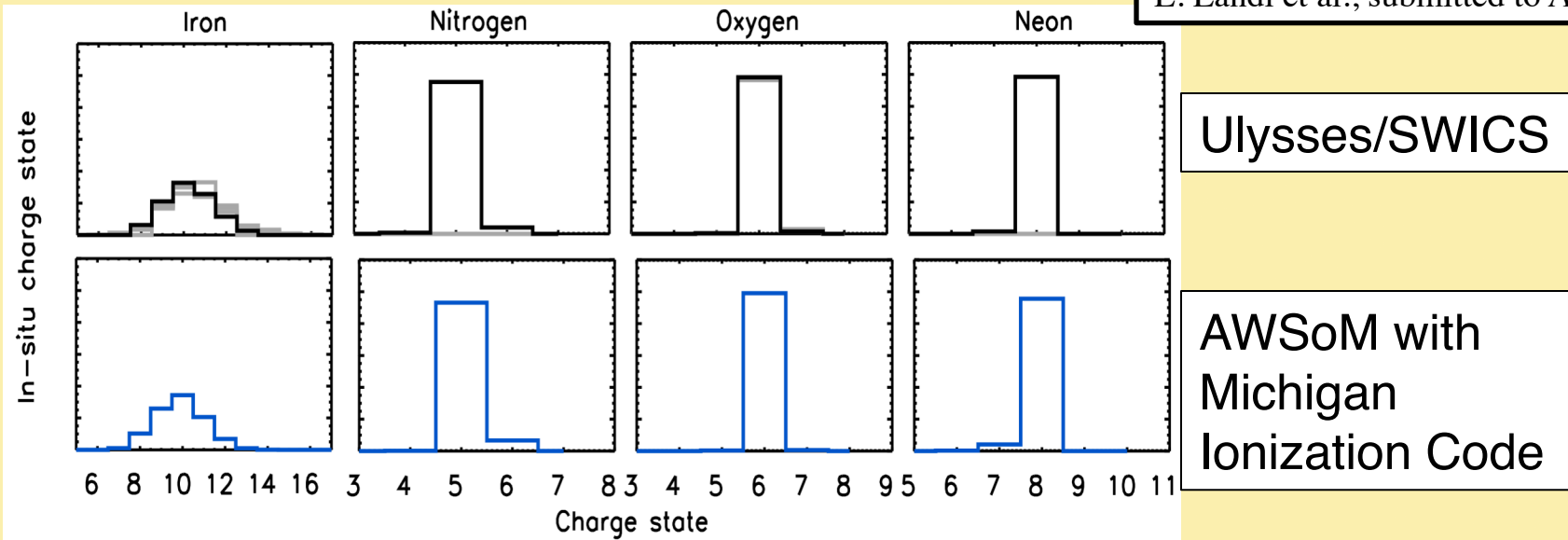
R. Oran et al., submitted to ApJ

M The electron density, temperature and bulk speed from the MHD model are used to derive charge state evolution along field lines, and compared to in-situ and remote observations



Validation: Charge State

E. Landi et al., submitted to ApJ



Ulysses/SWICS

AWSoM with Michigan Ionization Code

- M** In-situ Ulysses/SWICS (polar pass) charge state during minimum of solar cycle 23
- M** The close match in frozen-in charge states indicates that the model's coronal electron temperature, density and velocity are close to that of the solar corona

M AWSoM model for the solar corona and inner heliosphere:

- Alfvén wave turbulence with wave reflection
- Three-temperature (with proton temperature anisotropy)
- Validation studies with EUV images, ACE, STEREO A&B and Ulysses show that this model can capture many features of the solar corona and heliosphere

M AWSoM has just been transferred to CCMC for runs-on-request

- We are presently constraining the few model parameters to have good model-data comparison for all Carrington rotations.